August 1995 • NREL/TP-411-8246

Atomic-Scale Characterization of Hydrogenated Amorphous-Silicon Films and Devices

Annual Subcontract Report
14 February 1994 – 14 April 1995

A. Gallagher, D. Tanenbaum,
A. Laracuente, B. Jelenkovic
National Institute of Standards and Technology
Boulder, Colorado

NREL/TP-411-8246 • UC Category: 1262 • DE95009287

Atomic-Scale Characterization of Hydrogenated Amorphous-Silicon Films and Devices

Annual Subcontract Report
14 February 1994 – 14 April 1995

A. Gallagher, D. Tanenbaum,
A. Laracuente, B. Jelenkovic
National Institute of Standards and Technology
Boulder, Colorado

NREL technical monitor: W. Luft

National Renewable Energy Laboratory
1617 Cole Boulevard
Golden, Colorado 80401-3393
A national laboratory of the U.S. Department of Energy
Managed by Midwest Research Institute
for the U.S. Department of Energy
under contract No. DE-AC36-83CH10093

Prepared under Subcontract No. DAD-4-14084-01

August 1995

This publication was reproduced from the best available camera-ready copy submitted by the subcontractor and received no editorial review at NREL.

NOTICE

This report was prepared as an account of work sponsored by an agency of the United States government. Neither the United States government nor any agency thereof, nor any of their employees, makes any warranty, express or implied, or assumes any legal liability or responsibility for the accuracy, completeness, or usefulness of any information, apparatus, product, or process disclosed, or represents that its use would not infringe privately owned rights. Reference herein to any specific commercial product, process, or service by trade name, trademark, manufacturer, or otherwise does not necessarily constitute or imply its endorsement, recommendation, or favoring by the United States government or any agency thereof. The views and opinions of authors expressed herein do not necessarily state or reflect those of the United States government or any agency thereof.

Available to DOE and DOE contractors from:
Office of Scientific and Technical Information (OSTI)
P.O. Box 62
Oak Ridge, TN 37831
Prices available by calling (615) 576-8401

Available to the public from:
National Technical Information Service (NTIS)
U.S. Department of Commerce
5285 Port Royal Road
Springfield, VA 22161
(703) 487-4650

Printed on paper containing at least 50% wastepaper and 10% postconsumer waste

Preface

This report describes the results from the period April 15, 1994, to April 15, 1995, carried out by the National Institute of Standards and Technology (NIST) under contract DAD-4-14084-01 from the National Renewable Energy Laboratory. The research is carried out under the direction of Dr. Alan Gallagher, a NIST physicist, in the "JILA" research institute on the University of Colorado campus in Boulder, Colo. Under a subcontract with the University of Colorado, graduate students and postdoctoral students of the university work on the project. During the period covered by this report these students have been David Tanenbaum, who graduated in May 1995; Arnaldo Laracuente; Stefan Barzen, since September 1994; Punit Kalra, through January 1995; and Brana Jelenkovic, a part-time researcher.

Summary

Goal

The first objective of this work is to better understand the atomic-scale structure of glow-discharge–produced hydrogenated amorphous silicon (a-Si:H) films and devices, the character and causes of film structural inhomogeneities, and their effect on film and device quality. These films are known to be imhomogeneous, with many small regions of missing silicon that are generally thought to be deleterious to photovoltaic properties. We have been particularly interested in looking for the character and causes of these voids as they form at the growing film surface. The approach taken is to measure the morphology and chemical characteristics of the as-grown film surface with atomic-scale resolution by using a scanning tunneling microscope (STM). A second part of the program involves discharge-produced microparticulates, which may be a primary cause of film inhomogeneities. If these are depositing into the film, this is discernible in our STM data. We are also measuring discharge-produced particulates above the substrate by light scattering. A third effort is directed toward measuring voltage and band characteristics of cross-sectioned photovoltaic cells, versus light soaking and other parameters, by using the STM. This is directed toward diagnosing the characteristics of individual layers and junctions of working devices, to assist in device optimization.

Results

We have measured the topology of the surfaces of device-quality, intrinsic a-Si:H films deposited by rf discharge from silane in our laboratory. These have been studied as a function of film thickness and observed without air exposure. The results can be summarized by noting that the film surface is uniformly hilly, and as the film thickness increases from 1 to 100 nm, the surface rms roughness grows gradually, from ~0.35 to ~0.55 nm. The characteristic width of the surface hills increased more rapidly, from ~2 to ~4 nm. These results must be related to growth models to establish the consequences to film quality. However, these data are the first data of this kind, and the data set is too new to have generated such analysis yet within the modeling community.

The second issue addressed is possible incorporation of silicon particles into the growing film surface, where the particles form in the plasma above the substrate. We have discerned a significant deposition of 3–6 nm diameter particles, yielding a density in the film which could have severe consequences on film quality if the resulting voids act as carrier traps. This is a particularly important observation, since particles in the plasma are normally charged and thereby are not expected to reach the growing film surface. This is the first experiment capable of detecting these very small particles, and their presence in the film in large numbers has serious implications. They occupy about 0.01% of the film volume. This indicates that particle formation and growth are a much more severe problem for film quality than has been recognized. In a second component of this study, measuring larger particles in the plasma by light scattering, we have detected such particles primarily at the downstream exit of the discharge.

The third component of our research, to measure the properties of cross-sectioned cells with the STM, is in the development stage. We have so far constructed and tested an STM and sample manipulator specifically designed to allow these measurements. This includes precise sample positioning and the capability to minimize probe perturbations by using exceptionally low (~10 fA) tunneling currents.

TABLE OF CONTENTS

Page

Preface i

Summary ii

Introduction 1

Topology of a-Si:H surfaces 1

Deposition of plasma-produced particulates 8

Light-scattering observations 12

Apparatus for cross-sectioned PV cell diagnosis 14

Conclusions 14

References 16

Abstract 18

Figures

Fig. 1. Typical surface topologies of 1–50 nm thick films 3
Fig. 2. Typical surface topologies of 100 and 400 nm thick films 4
Fig. 3. Height correlation function versus film thickness 5
Fig. 4. Rms roughness and correlation length versus film thickness 6
Fig. 5. Diagrammatic representation of film growth over a particle 9
Fig. 6 STM images of particulates at the film surface 10
Fig. 7. Diagram of conformal film growth over a particulate 11
Fig. 8. Geometry of particulate scattering measurements 13
Fig. 9. Particulate scattering versus position in discharge 14
Fig. 10. Diagram of cross-sectioned cell setup and expected i-V signals 15

Introduction

The primary mechanisms and molecular species responsible for film growth in a silane discharge have been established (Doughty and Gallagher 1990; Doyle et al. 1990; Itabashi et al. 1990), but the ubiquitous character of particulate growth in the plasma is a relatively new discovery; some indications of its effect on film properties have been observed, but these are not well established (Howling et al. 1994; Schmidt et al. 1993). Part of the research reported here is directed toward an improved understanding of the role this dust plays in film quality and ways to mitigate deleterious effects.

Silicon particulates readily form in a-Si:H deposition discharges (Barnes et al. 1992; Bouchoule et al. 1991; Fukuzawa et al. 1994; Howling et al. 1991; Watanabe et al. 1990), as well as in Si dry-etching plasmas. They can cause some obvious deleterious effects, such as device failure or shorts when >0.3 μm diameter particles deposit on the substrate. However, they become negatively charged in the discharge, and this is expected to trap them in the plasma and prevent their incorporation into the growing film. Thus particles have only been expected to be a problem when the discharge is switched off and they can reach a surface. Previous measurement methods have not been capable of detecting much smaller particles, which might not behave in this manner. The most important result reported here is that very small particles do incorporate into the film during growth and may be the primary cause of film inhomogeneities. In addition to direct incorporation, particles suspended in the plasma affect the discharge, producing spatial inhomogeneities, discharge power and deposition rate variations, and changes in the types and energetics of species arriving at the substrate. We are studying these larger particles with light scattering, to delineate how they depend on conditions and if we can find ways to mitigate their presence.

Si voids in a-Si:H films are thought to be critical to photovoltaic properties and another component of the present program studies how voids arise at the growing surface. A scanning tunneling microscope (STM) is used to measure the surface characteristics of the as-grown film with atomic-scale resolution. During the previous year we concentrated on measuring the surface topologies of films grown at other facilities, for film thicknesses on the order of the 500 nm typically used in devices (Gallagher et al. 1994). This year we have concentrated on the dependence of surface topology on film thickness, starting with the initial (1 nm thick) layer up to 500 nm layers. These are essential data for understanding how voids and other inhomogeneities grow into the film, but more detailed film growth models are needed to use these data to clearly establish causes of these film imperfections.

In the third component of our research, we are developing the capability to measure the electrical properties of operating photovoltaics based on a-Si:H, by using the STM with cross-sectioned cells. This activity is in the development stage; progress in this apparatus development and testing is reported here.

Topology of a-Si:H surfaces

The initial atomic-scale morphology of a-Si:H deposited from a glow discharge will depend on the atomic-scale roughness and chemical composition of the substrate. To minimize the effect of such uncontrolled roughness and to optimize the connection to a large body of surface-science knowledge, we are currently studying a-Si:H film deposition onto oriented, nearly atomically smooth and clean surfaces of crystal Si. We prepare atomically flat crystal Si by heating an oxide-covered Si substrate in ultra high vacuum to >900 °C.

Our film-deposition region is designed and operated to mimic conditions and arrangements most commonly used to produce device-quality a-Si:H and alloy films by glow-discharge deposition. However, the special requirement of sample transfer into the STM necessitates some unusual arrangements; the sample is mounted

on a holder that is transferred between the discharge region and the STM. This holder also contains separate connections to two sides of the crystal to allow resistive heating during sample preparation. Also, the substrate surface is slightly above the plane of the grounded electrode, with some slightly recessed and protruding regions nearby. When film is deposited, the entire discharge region, shower head, and sample are heated to the substrate temperature. The rf electrode is 5 cm square and 1.6 cm from the substrate electrode, defining the discharge volume and yielding a relatively uniform discharge region at the sample. Deposition rate is measured with laser interference fringes and is normally 1–2 Å/s. This discharge geometry, with grounded surfaces adjacent to all sides of the rf electrode, is "asymmetric"; the rf and grounded electrode areas differ by a factor of 2. This ensures a uniform, efficient gas flow, but lowers the sheath potential and substrate ion bombardment compared to a symmetric discharge. Industrial systems are normally close to symmetric, as they utilize large electrode areas compared to the surface area (electrode length/gap »1). Diagrams of this apparatus can be found in our 1993 and 1994 Final Reports (Gallagher et al. 1993; Gallagher et al. 1994).

STM topography resolution on a rough surface is limited by the sharpness of the probe tip. Except where noted, for the present data the probe tip is sharper than any features on the surface, and the actual surface shape is recorded. The methods used to prepare these sharp probe tips and to establish their shape are described in our 1993 Final Report (Gallagher et al. 1993). The use of these unusually sharp tips provides the ability to ascertain if growing voids are present in the valleys of the film surfaces.

We have coated atomically flat and clean crystal Si with varying amounts of intrinsic a-Si:H in our deposition chamber and then measured the surface morphology of these films with our STM. As described in previous reports (Gallagher et al. 1993; Gallagher et al. 1994), we have made many checks to assure that these actually represent the surface of the a-Si:H; these will not be described again here. We have used standard, optimum conditions for depositing high-quality PECVD intrinsic films. We believe the morphologies presented here probably represent the types of microscopic morphologies that occur in most deposition chambers used to produce a-Si:H devices. As described in our 1994 final report (Gallagher et al. 1994), we have so far tested this issue only for 300–500 nm thick films grown at NREL, finding these surface morphologies similar but not identical to films of similar thickness from our laboratory.

The types of surface morphologies most often observed on films of increasing thickness are shown in Figs. 1&2. Here, in Figs. 1 and 2 (upper illustration), we show morphologies on 100 nm × 100 nm areas of four films of increasing thickness. The hills on the 400 nm thick film are so large that they are easier to see on the larger area shown in the lower illustration in Fig. 2. As can be seen in these figures, the surface height range and the lateral size of the surface hills continually grow with increasing film thickness. The valleys between the hills in these figures do not contain steep-sided void regions; this behavior was seen on all surface regions studied on these films (typically 50 regions per film). The general character (height, width, and steepness of hills) of these hilly regions is similar to those seen on earlier, 100–500 nm thick films reported on in our 1993 and 1994 final reports (Gallagher et al. 1993; Gallagher et al. 1994). But on those films some very different regions and some edges of exposed voids were observed, in contrast to the surfaces of the present films. We do not have a definite explanation of these changes, but we suspect they are due to subtle changes in the configuration of our discharge chamber and sample holder, which alter the incorporation of discharge-produced particulates into the films.

Figure 1 (facing page). Surface morphology of 1000 Å square areas of intrinsic a-Si:H films deposited at 0.17 nm/s and 250 °C from SiH_4 using PECVD in our laboratory, and transferred without vacuum exposure to a STM. Film thickness is 1.1 nm (upper), 4.5 nm (middle), and 50 nm (lower). In all figures the vertical scale has been expanded by a factor of three to assist viewing. ▶

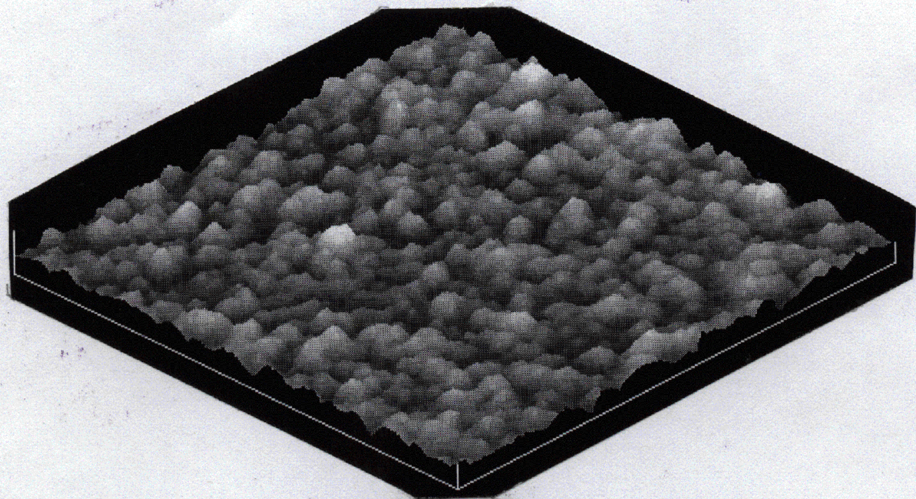
25Å

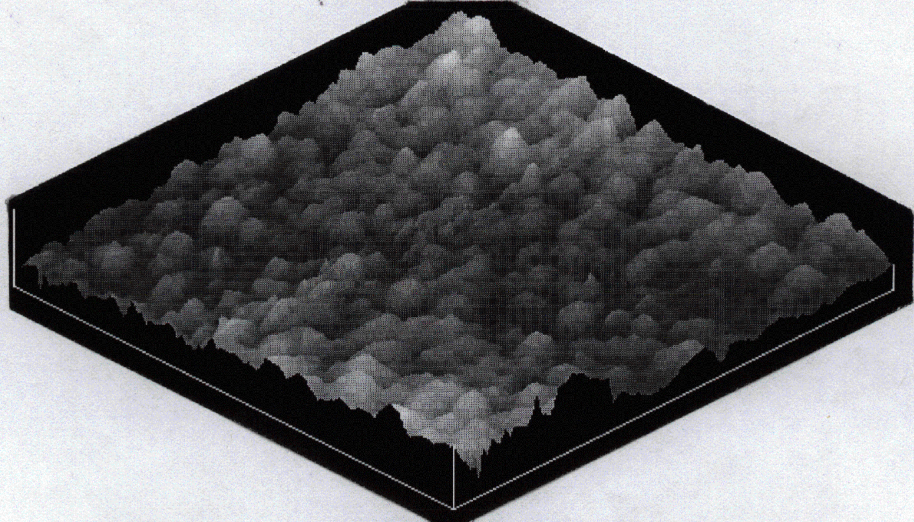
48Å

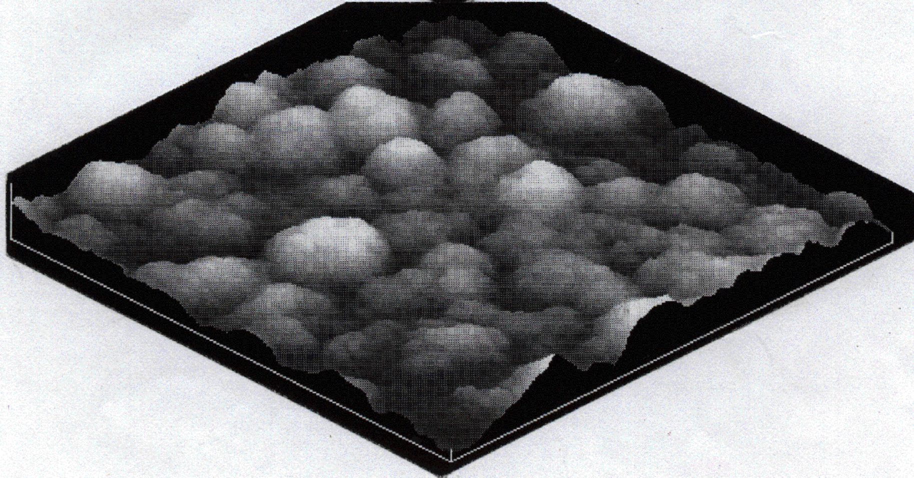
34Å

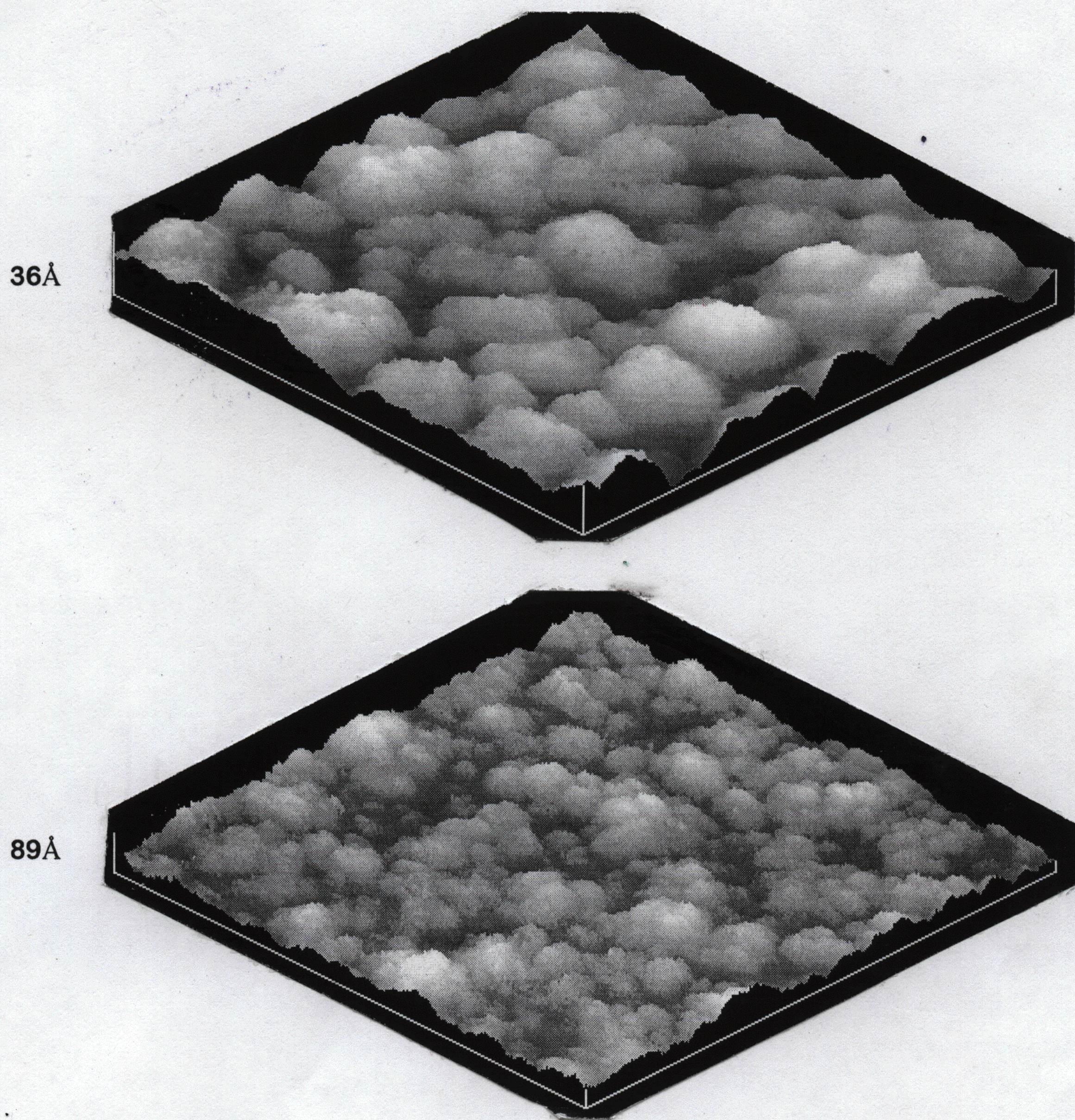

Figure 2. Surface morphology of 100 nm and 400 nm thick films, deposited as described in Fig. 1. (Upper) 100 nm × 100 nm area, vertically expanded by a factor of three, (lower) 400 nm × 400 nm area also expanded 3× vertically.

An effective way to describe the height range and lateral sizes of the surface hills seen in Figs. 1&2 is to plot the height correlation function, $G(r) = [h(x,y) - h(x',y')]^2$, averaged over the surface. Here x,y and x′,y′ are separated by r, and h(x,y) is the surface height at position x,y. This is done for several film thicknesses in Fig. 3, where the average over many surface regions is shown; relatively little scatter is seen when individual regions of a single film are compared. G(r) is the average height difference (squared) of points at lateral separation r. G(r) at large r is 2 times the rms surface roughness squared, whereas the r_c at which

$G(r_c) = G(\text{large } r)/2$ is the "correlation length" or characteristic radius of the surface hills. In Fig. 4 the average rms roughness and correlation length are plotted versus film thickness. The vertical bars in this figure represent the range of values obtained on typically 50 regions of each surface. The gradual rise in rms roughness and r_c with film thickness reflects the general behavior seen in Figs. 1&2.

Discussion

The density of a-Si:H films is typically 5% below the crystalline density, and the film typically contains ~10% hydrogen atoms. The simplest way to reconcile these properties is by postulating many small Si voids in the material, with H atoms bonded to the Si on the surfaces of these voids. Alternatively, there might relatively large regions with lower Si density, with H on dangling Si bonds within the region. NMR and SAXS studies confirm that we are dealing with such an inhomogeneous material (Family and Vicsek 1985; Gallagher et al. 1993; Gallagher et al. 1994; Gleason et al. 1987; McCaughey and Kushner 1989). The character of these voids may be crucial to the electronic properties and photovoltaic stability of these films, and finding the causes of void formation during film growth is a major concern. We are using these STM observations of the atomic-scale topography of the growing film surface to search for the exact character of these voids as they form and for their dependence on discharge conditions.

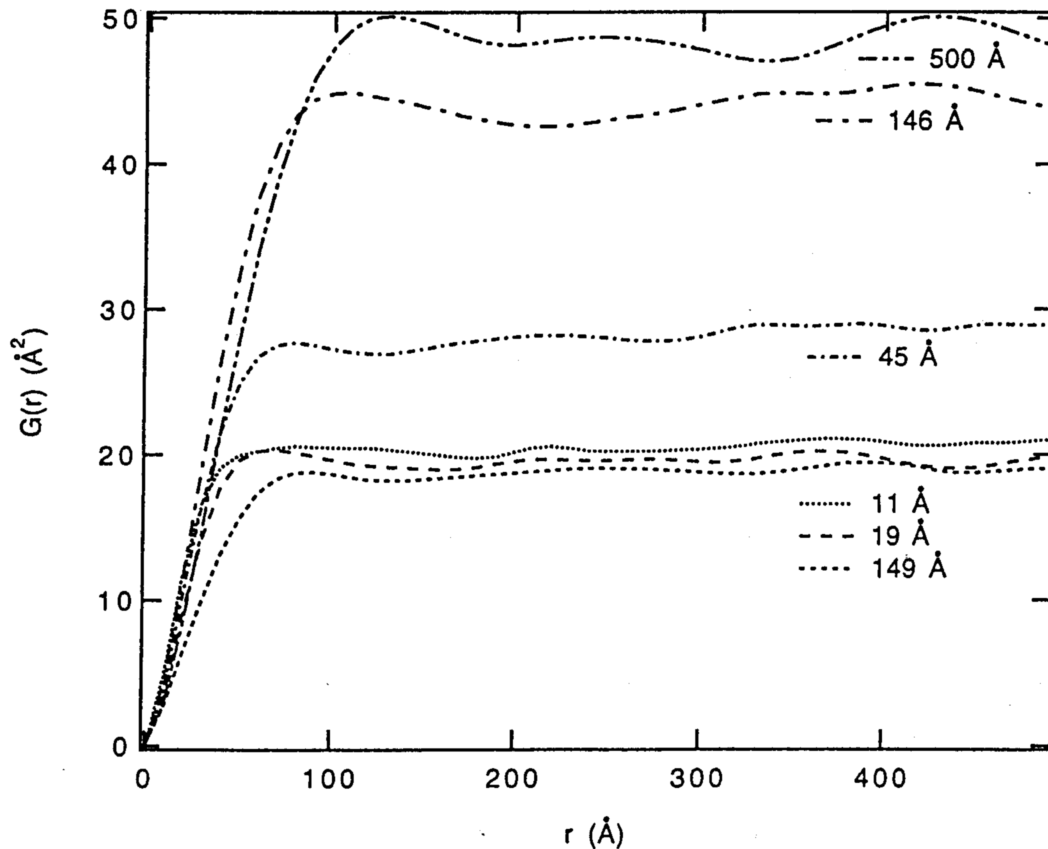

Figure 3. The averages of the height difference correlation functions for the films of different thicknesses.

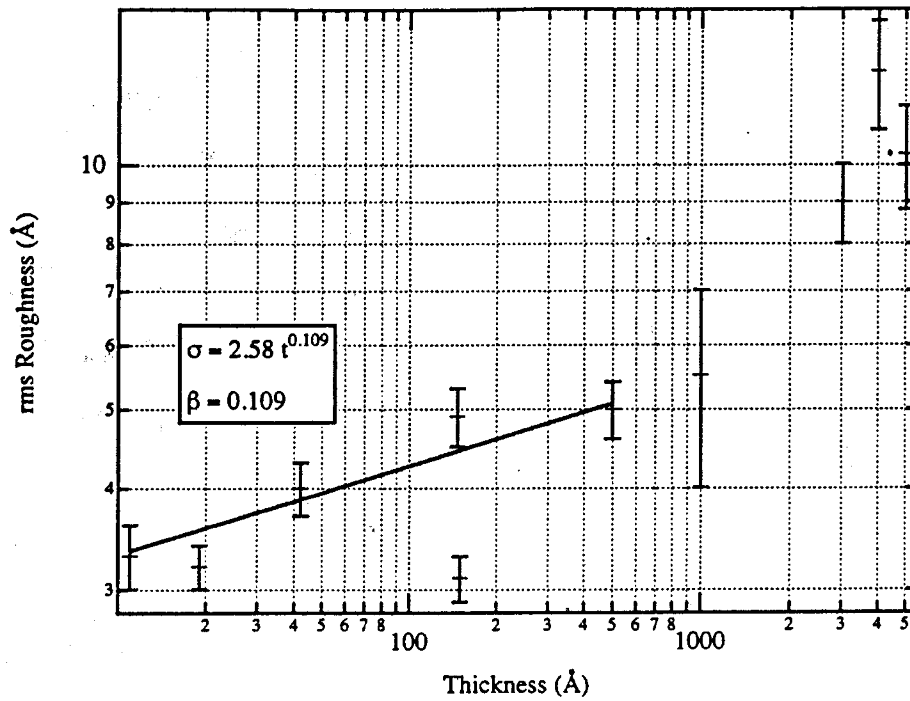

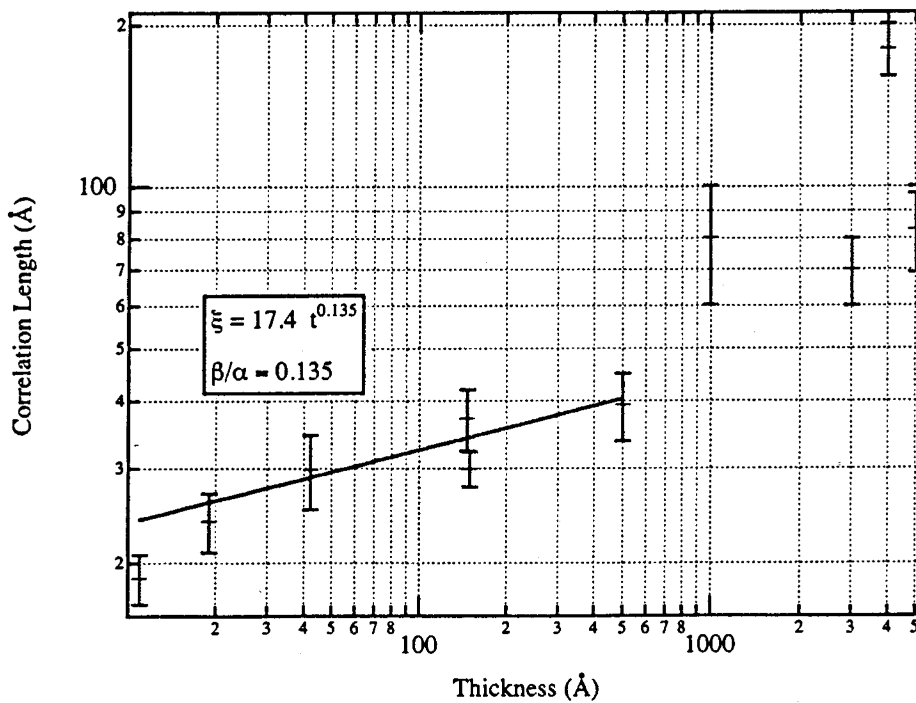

Figure 4. The rms roughness and correlation length as a function of film thickness for all the PECVD films studied. The error bars on the 1000 and 4000 Å thick films are not standard deviations, but ranges of observed values.

As reported in our 1993 Final Report (Gallagher et al. 1993), we have found growing void features on intrinsic films grown in our laboratory by rf PECVD, under conditions that yield conductivities and infrared absorption indicating good-quality film and that mimic typical-device preparation conditions. However, as described in our 1994 Final Report (Gallagher et al. 1994), we did not find such features on films prepared by rf PECVD at NREL. We searched many regions of the NREL films, particularly on the n-doped film, for the downward cusps that indicate a surface void, but we found only a few, in contrast to the films deposited in our chamber. Interestingly, we also found no smooth regions on the NREL films, again in contrast to the films produced in our laboratory. This year, we have studied thinner (1–50 nm) films deposited in our deposition chamber, and we have found these to be also essentially free of surface voids. In fact, they are uniformly hilly just like the NREL films, if one ignores the small fraction of images containing particulates. The rms height range and characteristic hill radius on the NREL films also looks like an expected extension of these thin film results, as can be seen in Fig. 4. Thus, it appears that the films grown in our deposition chamber develop excess surface irregularities as their thickness increases.

There are many subtle differences between the NREL deposition and that in our laboratory. The NREL chamber is a 4 inch cross with the substrate above and the rf electrode below the center. Only the substrate is directly heated to T_S, although the rf electrode generally rises to ~1/2 of the substrate temperature in such an arrangement. In our chamber all surfaces around and upstream of the substrate are heated to T_S, and the substrate and rf electrode are vertical. The edges of the rf electrode in the NREL chamber are some distance from a surrounding screen, so that it forms a moderately asymmetric discharge. Grounded surfaces are very close to the rf electrode in our chamber, so it is a more asymmetric discharge. One consequence of this is that lower surface ion-bombardment energies occur in our system, for a given discharge power density or film deposition rate. The substrate in our system is also on a removable holder, producing a local irregularity in the substrate surface; this can affect where discharge-produced, negatively charged silicon particulates reside in the discharge (Howling et al. 1994). The silane pressure, deposition rate, and electrode gap are very similar in the two chambers. The silane mass flow in the NREL deposition is 3 times what we use, but the cross section is also ~3 times as large so the flow speed is probably similar. It is not known with certainty which, if any, of these differences is critical, but the fact that very different film properties are obtained from these very similar deposition conditions shows that these poorly understood, subtle differences can be very important.

Mechanisms and causes of topology

The "dynamical scaling" model for epitaxial surface growth is a mathematical model whose parameters can be adjusted to produce approximately the observed character of surface morphology versus film thickness (Family and Vicsek 1985). However, this does not address the question of what physical processes are occurring and how they affect the film semiconducting properties. A few calculations exist that consider film or epitaxial growth subject to both shadowing and surface diffusion, but these contain various restrictive assumptions and limited numbers of actual examples (McCaughey and Kushner 1989). We are currently looking for physical models for the growth process that can explain the data. As an example, it is possible that initial, closely spaced nucleation sites on the initial surface grow into the small hillocks in the 1.1 nm film. These then fill in and smooth out with further growth, owing to surface diffusion of depositing SiH_3 radicals. However, a simple diffusion model would lead to a continually decreasing height range as the film grows over the initial roughness that resulted from initial nucleation. This disagrees with the data, and it also fails to include the very important roughening effect of shadowing. Another possibility is that new sites of comparatively rapid or slow growth may be continually started randomly on the surface, producing the observed, slowly growing height of the surface roughness. Another possibility is that the continual deposition of nanoparticulates could produce the surface roughness.

It is well established that a-Si:H film growth from silane glow discharge results predominantly from neutral radical reactions with the film surface (Doughty and Gallagher 1990; Doyle et al. 1990; Itabashi et al. 1990). These radicals, primarily SiH_3, arrive at the surface in a cosine distribution, and so they strike protruding regions of the surface more frequently than low regions. If they reacted and remained at the point of arrival, this microscopic shadowing combined with the incident angular distribution would inevitably lead to a highly porous, filamentary, and useless film (Gleason et al. 1987). Since this is not observed, either radical surface diffusion before incorporation occurs or energetic surface ion bombardment erodes away protruding features of the growing film. Although energetic bombardment can occur for some deposition conditions, the highest (electronic) quality films are grown in low-power rf, higher-frequency or triode discharges that yield minimal energetic bombardment of the film. Thus, it is clear that considerable radical surface diffusion must occur and moreover that this diffusion must be accompanied by some degree of preferential incorporation in valleys as opposed to hilltops. Such a preference, which is often described as a variation in chemical potential, is logical since the concave character of the valleys offers more bond sharing or multiple bonding than on the convex hilltops. The necessary radical diffusion, as well as a dangling-bond "radical" diffusion, is also reasonably explained by the inability of SiH_3 to insert exothermically into an H passivated surface.

It is expected that shadowing, combined with surface diffusion and reactions of depositing SiH_3, can produce a surface covered with hills. Presumably the hill steepness results from competition between shadowing and the difference in incorporation probability between the valleys and hilltops. It has previously been postulated that the characteristic hill separation ($2r_c$) is related to the typical SiH_3 diffusion distance before incorporation, but the data in Figs 1–4 demonstrate that there is no unique value for r_c; it continually increases with film thickness. This result is not explained by any physically meaningful models for film growth, and it is too early to offer any conjectures here regarding its causes. The competition between shadowing and surface diffusion with preferential incorporation in valleys can nonetheless be postulated as the cause of the hilly regions seen most frequently on all films. However, it does not explain the void regions and inhomogeneities we observe on the thicker films from our deposition chamber, nor does it explain the many voids implied by SAXS, NMR, and density measurements on all films. In our 1994 Final Report (Gallagher et al. 1994) we suggested a variety of phenomena that could cause these voids and differences between films from different deposition chambers. We will not repeat these here, except to note that we now have direct evidence that one of these, particulate incorporation during growth, does indeed occur. This is discussed in the next section.

Deposition of plasma-produced particulates

Silicon particles are seen by light scattering in almost all silane discharges where such observations are made. These particles generally have diameters of 50–1000 nm. A yellow powder deposited downstream is another sufficient, but not necessary, indicator of particles formed in the discharge. These particulates become negatively charged in the discharge, and discharge sheath fields prevent negatively charged particles from reaching the substrate as long as the discharge is on. When the discharge is terminated, these particles are subject primarily to a gas flow force in the downstream direction and to a thermophoresis force toward the colder surfaces. Since the substrate is normally the hottest surface in the discharge region, particles generally do not deposit on the substrate after discharge termination. However, smaller particulates (1–20 nm in diameter) carry a small number of negative charges, and it appears possible that they may occasionally become neutralized or positively charged and thereby reach the substrate during discharge. If this were true, it could have serious consequences for film quality, as the particle-film boundaries probably contain carrier trap sites and shadowing effects induce film voids. The manner in which this is expected to occur is shown in Fig. 5. Since the depositing species arrive in a cosine distribution about the surface normal, the regions below the particle edges grow more slowly than elsewhere, producing the propagating voids suggested there.

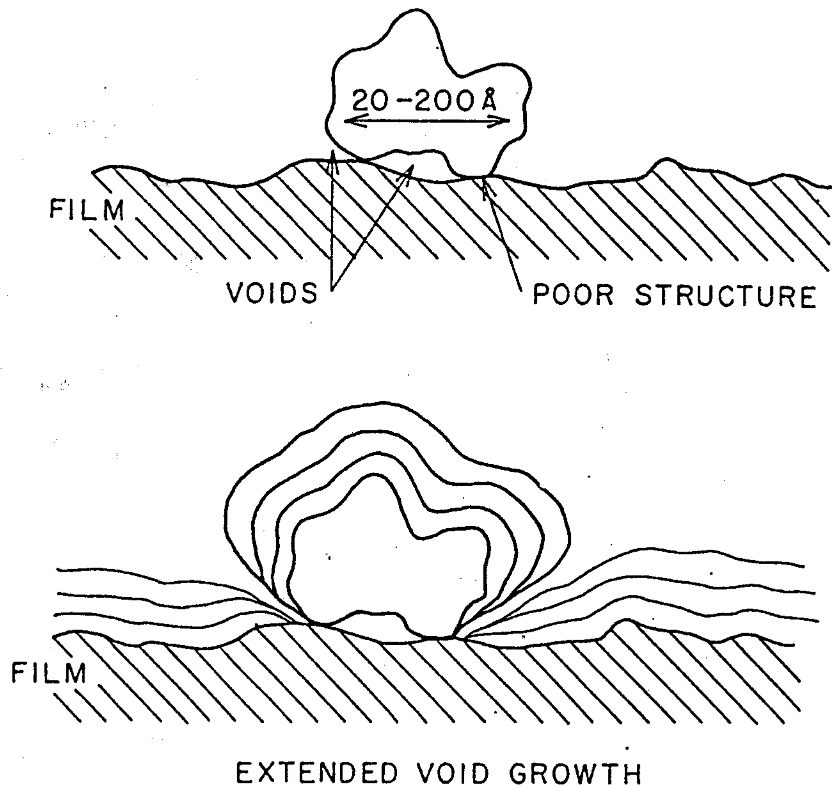

Figure 5. Diagrammatic representation of the effects of incorporation of a small particle into a growing film. The lower figure shows the expected effect of shadowing on the growth of successive layers of film.

Particles smaller than 30 nm have never been seen in the plasma, on the film surface, or in the films, but it is not clear if anyone has had the ability to detect them if they were present. They are not detectable in the vapor or on the surface by light scattering, since the scattering cross section for small particles varies as the sixth power of the radius. Here we report clear proof that small particles continually deposit onto the growing surfaces of a-Si:H films, for films deposited in our laboratory by the rf PECVD method using standard conditions that are utilized at all facilities to produce optimum-quality films.

Our deposition system and the scanning tunneling microscope (STM) analysis of film surfaces has been described in previous reports and publications (Gallagher et al. 1993; Gallagher et al. 1994). The films reported here were deposited at 0.1–0.2 nm/s, 250 °C, 0.5 torr silane, and 1.9 cm electrode gap with sufficient flow to yield less than 5% fractional silane depletion (i.e., optimum conditions). Our entire deposition chamber is at 250 °C, in contrast to most systems where only the substrate is directly heated. This eliminates any uncertainty regarding the actual substrate temperature and gas density, but may enhance particulate deposition on the substrate. A thermophoresis force that pushes neutral particles toward colder surfaces is absent in our uniform temperature system.

As described in the previous section, we have studied the topology of a-Si:H films deposited on atomically flat, H-terminated crystal silicon substrates, versus film thickness. For films of ≤50 nm thickness we observe on most images uniformly hilly surface topologies with an rms height variation of 0.3–0.6 nm. This thickness variation appears as rolling hills, primarily with side slopes not exceeding 35 degrees. However, we occasionally observe a much larger hill standing out from this comparatively flat topology; three examples are shown in Fig. 6. These larger hills, which are typically ~10 nm diameter,

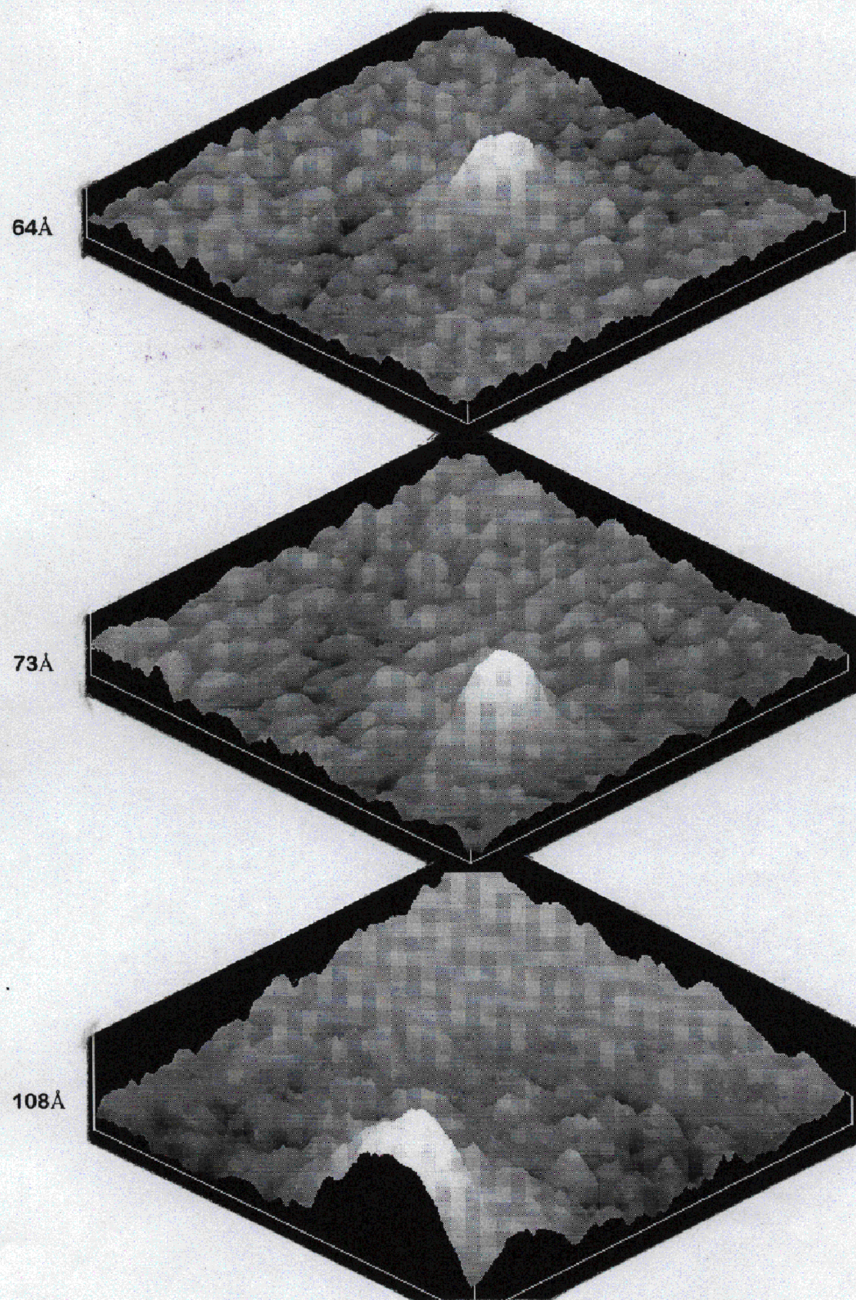

Figure 6. STM images of film surface topologies, showing particulates deposited onto the growing film surface. The average film thickness is 1.9 nm in the top image, 4.5 nm for the middle image, and 14.5 nm for the bottom image.

cover about 1% of the total surface area studied. They are not the tail of a broad distribution of hill sizes, as they stand out clearly from the general topology that results from the incorporation of individual radicals into the film (i.e., these isolated lumps must be particulates deposited on the surface during or after film growth). This is a crucial difference, as continuous deposition of small particulates into the growing film could have very deleterious effects on its PV behavior, whereas such small particulates deposited only on the fully grown film would be relatively benign. The evidence and reasoning that lead us to believe these are deposited during the discharge is presented next.

Although we do not remove the samples from the vacuum chamber between deposition and STM analysis, it is possible that particulates from the chamber surfaces could deposit on the samples during sample transfer into the STM. There are several reasons why we do not think this is the source of the detected particulates. First, such particulates will not be well adhered to the film surface, and the STM probe would be likely to push them around rather than scan smoothly and repeatedly over them, as seen in the images. Next, we would expect to see a much larger range of particle sizes, particularly larger particles, compared to the 3–9 nm diameter range actually observed. Next, the widths of the recorded bumps are larger than that expected for a round particle scanned by our STM probe. The expected result for a round particle is indicated in the top half of Fig. 7; there one sees that the observed width is the sum of the bump and probe widths and the bump height is preserved. We measure our probe width using silicon nanocolumns, as described in our 1993 report (Gallagher et al. 1993), so we know the probe contribution to width and conclude that most of the image broadening is due to the object rather than the probe. The effect of conforming layered growth is shown in Fig. 5 (lower); note that this broadens while preserving height. The recorded broadened bump shapes are consistent with this phenomenon. Next, we have observed an increase in bump density and average bump width with increasing film thickness; again this is consistent with a steady deposition of particulates and conformal covering as shown in the lower part of Fig. 7. These observations also apply to the possibility that particles suspended in the discharge are deposited when the discharge is turned off, as might be expected for

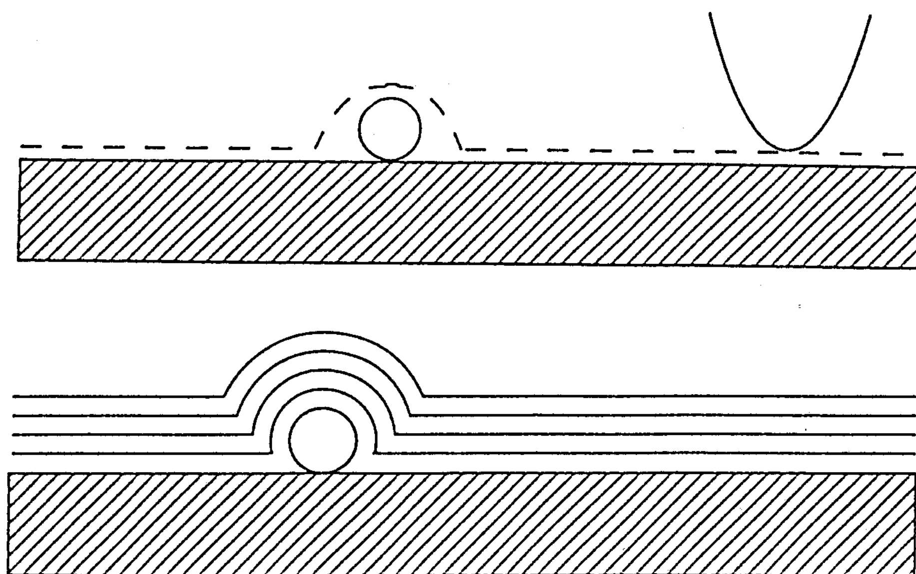

Figure 7. Diagrammatic representation of the expected STM image (dashed line in the top figure) of a round particle on a flat surface. The lower figure shows successive shapes of the surface that results from the conformal film growth onto a round particle on a flat surface. This type of growth, as well as the shadowed growth of Fig. 5, leads to a widening of the feature, but preserves the height of the particle.

negatively charged particles. Again, we would expect this to deposit a large range of sizes, in contrast to what is observed. As an additional test we have deposited some layer thicknesses with one versus multiple terminations of the discharge. If particles were being deposited after each discharge termination, we would expect to observe fewer particles on the continuously deposited film. We observed no significant variations in particle size or density. We conclude, from this preponderance of evidence, that we are observing small silicon particulates that have grown in the plasma and deposited on the substrate during film growth.

Discussion

Particulate formation in a silane discharge and deposition onto the substrate is very poorly understood. It should depend on many discharge parameters, including factors such as the shapes of electrode surfaces and edges that are not normally considered. Thus, the present results do not apply universally. However, they do suggest that particulate deposition during film growth may be a major film quality factor, which has not previously been recognized. The particles we have observed fill about 0.01% of the film volume, an amount that could have very significant consequences on electrical properties or trap densities. Extended voids as suggested in Fig. 5 could increase the affected volume. A number of methods for mitigating particulate growth in discharges have been suggested or studied, and the present observations suggest that it may be worthwhile to try some of these and monitor their effect on film quality.

Silicon microparticulates grow in the plasma under many silane discharge conditions, particularly as power is increased or gas flow is decreased (Howling et al. 1994). Their presence is most often revealed as yellow powder downstream from the deposition chamber, particularly at pumping orifices and insulators. This results from the agglomeration of many small particles into larger (μm) sizes as the gas carries the particulates downstream. The larger particles more efficiently absorb and fluoresce radiation, per unit mass, and more readily deposit out, thereby signaling the presence of the smaller, less visible particles in the deposition chamber. As particles within the plasma grow in size, to a few nm or so, they become negatively charged owing to the much higher electron versus ion velocities in the discharge. The plasma is positively biased relative to the surfaces, so these negative ions are trapped in the discharge. The charge is proportional to the radius, so particles can grow to large dimensions within the plasma under some conditions. However, under typical high flow, low power conditions used to produce device-quality films, most particles escape at the downstream edge of the plasma before reaching μm sizes. There the sheath fields are weaker, and the gas flow drags them away once they reach sufficient size. (The gas drag force and the electrostatic force are proportional to diameter squared and diameter, respectively.) Although discharge models have not considered the problem, it appears feasible that the smaller particles, which carry only a few charges on average, may occasionally be neutralized and escape to the substrate during the discharge. Of course, when the discharge is turned off, particles will move under a combination of gravitational, gas drag, and thermophoretic forces, which may allow even large particles to land on the substrate.

Light-scattering observations

Light scattering from silicon particulates in silane discharges has been carried out in a variety of laboratories, but few measurements are made under "device quality" deposition conditions and the observations have not been correlated with film properties (e.g., Barnes et al. 1992; Bouchoule et al. 1991; Fukuzawa et al. 1994; Howling et al. 1991; Howling et al. 1994; Schmidt et al. 1993; and Watanabe et al. 1990). In addition, the amount and location of particulates are highly dependent on the details of each individual deposition chamber. We have therefore set up light-scattering observations for a discharge chamber that is as close as possible to that with which we produce films for STM studies. Unfortunately, it is not possible to utilize exactly the same discharge configuration, since we need a transparent side window and a-Si:H coatings deposit on unprotected windows, attenuating the scattered light signal. Thus, we use a set of thin metal vanes to protect the observation windows from this coating, as shown in Fig. 8. Since these vanes are electrically floating,

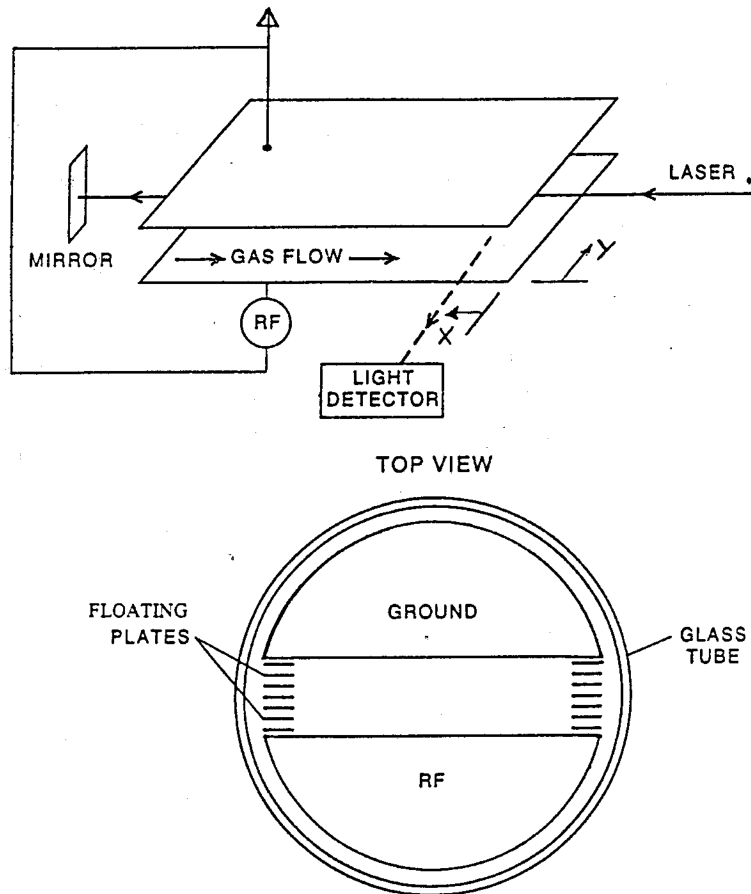

Figure 8. Experimental arrangement for particulate scattering measurements.

their inherent capacitances assist in dividing the discharge voltage equally between them, thereby minimizing their effect on the discharge. A view of the discharge emission from the downstream end confirms this.

Our observations of light scattering have been done mostly in the configuration shown at the top of Fig. 8. A typical result is shown in Fig. 9, where the electrode position relative to the data is shown below the graph. We have not measured the size distribution of the particles responsible for this light scattering, but from the literature and scattering cross sections we estimate 100–1000 nm. These are probably accompanied by many more small particles that are not observed by light scattering. Note that the scattering peaks downstream of the end of the electrodes and grows rapidly with decreasing gas flow. For this particular pressure and discharge power, the scattering decreased with increasing temperature, but this is not always seen. Changes in the tubing configuration several centimeters downstream also affects the gas flow pattern, and with it the pattern of dust scattering signals. It is hard to generalize the rather complex results, but usually there is relatively little light scattering from the discharge volume under flow and power conditions used to produce the STM studied films. As already noted, measuring light scattering by the actual particles detected by the STM is not feasible, and these scattering signals are indirect evidence of their presence, as seen downstream where particle agglomeration has occurred. Our only conclusion from these preliminary observations is that particles are clearly present under our normal deposition conditions. It is worthwhile to note that we utilize the same deposition rate; hence power density, typically used for producing device-quality films, and our flow velocities are very high by normal standards (large mass flow/tubing area). Thus we suspect that particulates are present in most or all silane PECVD chambers.

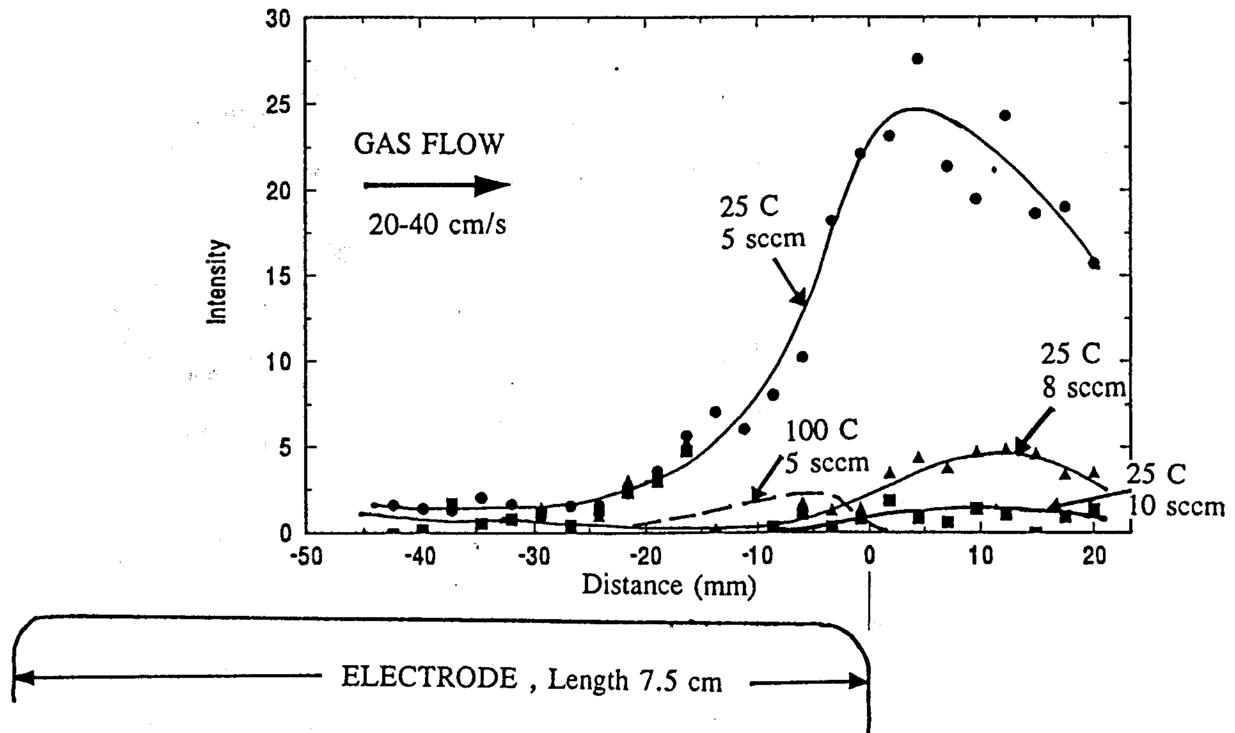

Figure 9. Mie scattering versus distance from end of electrodes.

Apparatus for cross-sectioned PV cell diagnosis

STM measurements of cross-sectioned superlattices are now a well-established technique (Smith et al. 1995). The changes in band gap and band edge voltage are seen with STM current-voltage spectroscopy. We are arranging to do this on a-Si:H photovoltaic cells, in the dark or while under illumination, to ascertain the characteristics of junctions and quasi-fermi levels before and after light soaking. The setup and the expected current voltage relations are shown diagrammatically in Fig. 10. We have now constructed an STM stage that has the required precise sample positioning control to allow tunneling at the ~1 μm wide exposed cell surface. It also allows precise positioned light illumination of the sample. We have also developed a sample holder that allows cleaving cells in vacuum and that contains the necessary two-sample contacts. Finally, we have developed an in-vacuum amplifier capable of measuring the STM current voltage relation at currents as low as 10 fA. The principal remaining issue that must be solved to allow the measurements is possible band pinning by surface states that result from the cleave. To address this possibility, we plan to hydrogenate the exposed surface with H atoms from a hot tungsten filament.

Conclusions

It is apparent that STM images can distinguish unique aspects of and differences between a-Si:H films and can discern both large-scale and small-scale film imhomogeneities. They can also detect the deposition of small particulates from the discharge that are so far not detectable by any other means. The most important observation we have made with this capability is that small (3–6 nm diameter) silicon particles are being deposited onto the film surface and incorporated into the film during growth. A second result is the steady growth in both rms roughness and roughness correlation length (hill width) with increasing film thickness. We can be pretty certain that the particle incorporation, inevitably accompanied by microvoids, has a

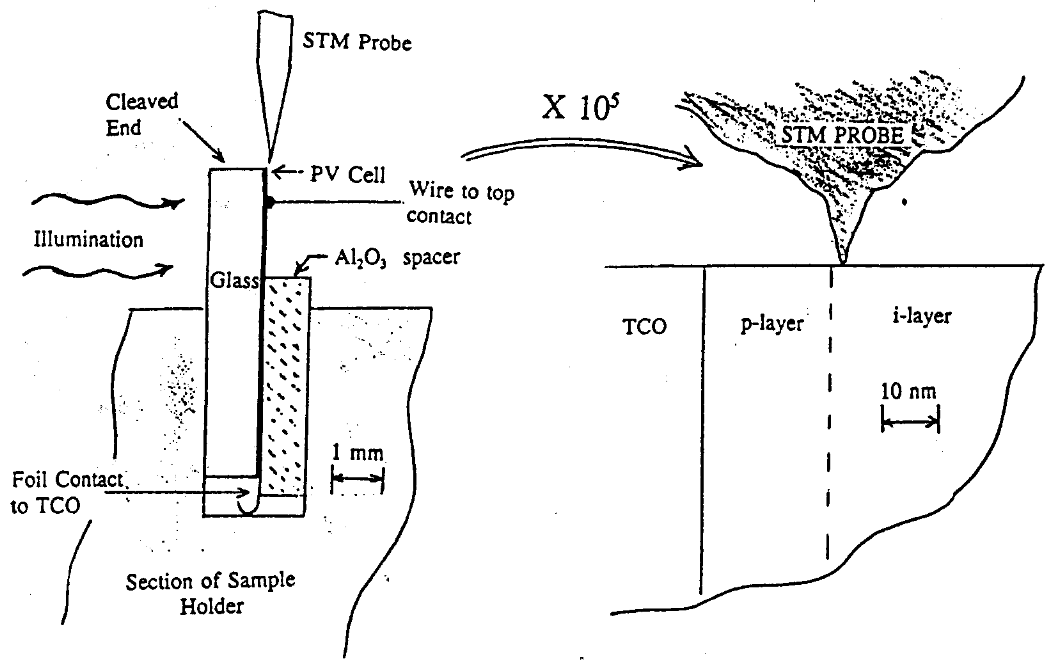

Diagram of the experimental arrangement

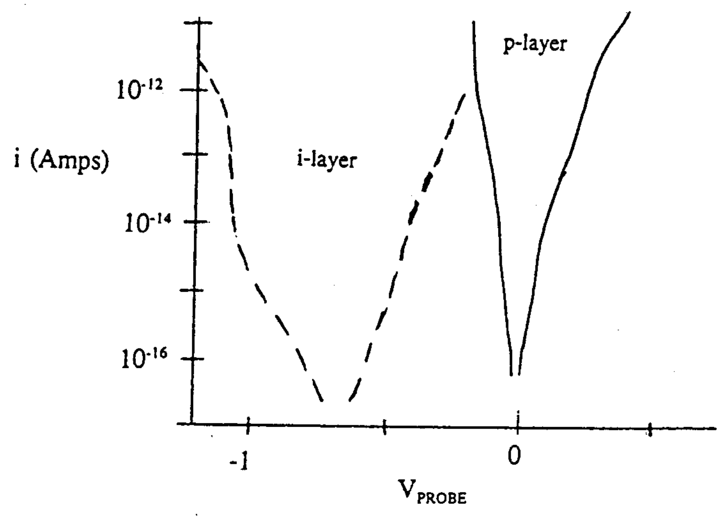

Figure 10. Example of the expected STM, i-V signals.

deleterious effect on film electronic properties, but we must await better growth models to ascertain the consequences of the changing surface topology.

Since an STM study of one surface requires several days of preparation and diagnosis and does not provide information on the growth of particles, we are also utilizing light scattering to obtain more immediate data regarding how discharge conditions and apparatus configurations affect particles suspended in the plasma. This detects larger particles than those we have found in the film surface, using the STM, but it appears likely that the larger particles are useful tracers of the smaller particles which that reach the film surface.

References

Barnes, M.S.; Keller, J.H.; Forster, J.C.; O'Neill, J.A.; Coultas, D.K. (20 January 1992). "Transport of Dust Particles in Glow-Discharge Plasmas." Phys. Rev. Lett. (68:3); pp. 313-316.

Bouchoule, A.; Plain, A.; Boufendi, L.; Blondeau, J. Ph.; Laure, C. (15 August 1991). "Particle Generation and Behavior in a Silane-Argon Low-Pressure Discharge Under Continuous or Pulsed Radio-Frequency Excitation." J. Appl. Phys. (70:4); pp. 1991-2000.

Doughty, D.A.; Gallagher, A. (1 January 1990). "Spatial Distribution of *a*-Si:H Film-Producing Radicals in Silane RF Glow Discharges." J. Appl. Phys. (67:1); pp. 139-145.

Doyle, J.R.; Doughty, D.A.; Gallagher, A. (1 November 1990). "Silane Dissociation Products in Deposition Discharges." J. Appl. Phys. (68:9); pp. 4375-4384.

Family, F.; Vicsek, T. (1 February 1985). "Scaling of the Active Zones in the Eden Process on Percolation Networks and the Ballistic Deposition Model." J. Phys. A: Math. Gen. (18:2); pp. L75-L81.

Fukuzawa, T.; Shiratani, M.; Watanabe, Y. (6 June 1994). "Novel *In Situ* Method to Detect Subnanometer-Sized Particles in Plasmas and Its Application to Particles in Helium-Diluted Silane Radio Frequency Plasmas." Appl. Phys. Lett. (64:23); pp. 3098-3100.

Gallagher, A.; Tanenbaum, D.; Laracuente, A.; Kalra, P. (July 1994). *Growth Mechanisms and Characterization of Hydrogenated Amorphous-Silicon-Alloy Films, Final Subcontract Report, 15 February 1991—14 April 1994.* NREL/TP-411-6864. NTIS Accession No. DE94011842. Golden, CO: National Renewable Energy Laboratory.

Gallagher, A.; Tanenbaum, D.; Laracuente, A.; Molenbroek, E. (August 1993). *Growth Mechanisms and Characterization of Hydrogenated Amorphous-Silicon-Alloy Films, Annual Subcontract Report, 14 February 1992—13 February 1993.* NREL/TP-411-5749. NTIS Accession No. DE93018202. Golden, CO: National Renewable Energy Laboratory.

Gleason, K.K.; Wang, K.S.; Chen, M.K.; Reimer, J.A. (15 April 1987). "Monte Carlo Simulations of Amorphous Hydrogenated Silicon Thin-Film Growth." J. Appl. Phys. (61:8); pp. 2866-2873.

Howling, A.A.; Hollenstein, Ch.; Paris, P.-J. (16 September 1991). "Direct Visual Observation of Powder Dynamics in RF Plasma-Assisted Deposition." Appl. Phys. Lett. (59:12); pp. 1409-1411.

Howling, A.A.; Sansonnens, L.; Dorier, J.-L.; Hollenstein, Ch. (1 February 1994). "Time-Resolved Measurements of Highly Polymerized Negative Ions in Radio Frequency Silane Plasma Deposition Experiments." J. Appl. Phys. (75:3); pp. 1340-1353, and references therein.

Itabashi, N.; Nishiwaki, N.; Magane, M.; Naito, S.; Goto, T.; Matsuda, A.; Yamada, C.; Hirota, E. (March 1990). "Spatial Distribution of SiH_3 Radicals in RF Silane Plasma." Jpn. J. Appl. Phys. (29:3); pp. L505-L507.

McCaughey, M.J.; Kushner, M.J. (1 January 1989). "Simulation of the Bulk and Surface Properties of Amorphous Hydrogenated Silicon Deposited from Silane Plasmas." J. Appl. Phys. (65:1); pp. 186-195.

Schmidt, U.I.; Schröder, B.; Oechsner, H. (11 December 1993). "Influence of Powder Formation in a Silane Discharge on a-Si:H Film Growth Monitored by *In Situ* Ellipsometry." Proceedings of the Fifteenth International Conference on Amorphous Semiconductors - Science and Technology, September 6-10, 1993, Cambridge, England. J. Non-Cryst. Solids (164-166:1); pp. 127-130.

Smith, A.R.; Chao, K.-J.; Shih, C.K.; Shih, Y.C., Streetman, B.G. (23 January 1995). "Cross-Sectional Scanning Tunneling Microscopy Study of GaAs/AlAs Short Period Superlattices: The Influence of Growth Interrupt on the Interfacial Structure." Appl. Phys. Lett. (66:4); pp. 478-480.

Watanabe, Y.; Shiratani, M.; Makino, H. (15 October 1990). "Powder-Free Plasma Chemical Vapor Deposition of Hydrogenated Amorphous Silicon with High RF Power Density Using Modulated RF Discharge." Appl. Phys. Lett. (57:16); pp. 1616-1618.